Improving Multimodel Forecasts of the Vertical Distribution of Heating Using the TRMM Profiles

T. N. KRISHNAMURTI, ARINDAM CHAKRABORTY,* AND A. K. MISHRA

Department of Meteorology, The Florida State University, Tallahassee, Florida

(Manuscript received 6 October 2008, in final form 29 August 2009)

ABSTRACT

Recently the National Aeronautics and Space Administration (NASA) Tropical Rainfall Measuring Mission (TRMM) project office made available a new product called the convective–stratiform heating (CSH). These are the datasets for vertical profiles of diabatic heating rates (the apparent heat source). These observed estimates of heating are obtained from the TRMM satellite's microwave radiances and the precipitation radar. The importance of such datasets for defining the vertical distribution of heating was largely the initiative of Dr. W.-K. Tao from NASA's Goddard Laboratory. The need to examine how well some of the current cumulus parameterization schemes perform toward describing the amplitude and the three-dimensional distributions of heating is addressed in this paper. Three versions of the Florida State University (FSU) global atmospheric model are run that utilize different versions of cumulus parameterization schemes; namely, modified Kuo parameterization, simple Arakawa–Schubert parameterization, and Zhang–McFarlane parameterization. The Kuo-type scheme used here relies on moisture convergence and tends to overestimate the rainfall generally compared to the TRMM estimates. The other schemes used here show only a slight overestimate of rain rates compared to TRMM; those invoke mass fluxes that are less stringent in this regard in defining cloud volumes. The mass flux schemes do carry out a total moisture budget for a vertical column model and include all components of the moisture budget and are not limited to the horizontal convergence of moisture. The authors carry out a numerical experimentation that includes over a hundred experiments from each of these models; these experiments differ only in their use of the cumulus parameterization. The rest of the model physics, resolution, and initial states are kept the same for each set of 117 forecasts. The strategy for this experimentation follows the authors' previous studies with the FSU multimodel superensemble. This includes a 100-day training and a 17-day forecast phase, both of which include a large number of forecast experiments. The training phase provides a useful statistical database for tagging the systematic errors of the respective models. The forecast phase is designed to minimize the collective bias errors of these member models. In these forecasts the authors also include the ensemble mean and the multimodel superensemble. In this paper the authors examine model errors in their representations of the heating (amplitude, vertical level of maximum, and the geographical distributions). The main message of this study is that some cumulus parameterization schemes overestimate the amplitude of heating, whereas others carry lower values. The models also exhibit large errors in the placement of the vertical level of maximum heating. Some significant errors were also found in the geographical distributions of heating. The ensemble mean largely mimics the model features and also carries some large errors. The superensemble is more selective in reducing the three-dimensional collective bias errors of the models and provides the best short range forecasts, through hour 60, for the heating. This study shows that it is possible to diagnose some of the modeling errors in the heating for individual member models and that information can be important for correcting such features.

1. Introduction

In the course of examining model-simulated vertical distribution of heating (Q_1) and moistening (Q_2), several authors expressed concerns about possible modeling errors in the amplitude and in the placement of the vertical levels of maximum heating or moistening (Tao et al. 2007). Such errors may stem from choice

* Current affiliation: Centre for Atmospheric and Oceanic Sciences, Indian Institute of Science, Bangalore, India.

Corresponding author address: T. N. Krishnamurti, Department of Meteorology, The Florida State University, Tallahassee, FL 32306.
E-mail: tnk@io.met.fsu.edu

DOI: 10.1175/2009JCLI2878.1

TABLE 1. List of acronyms used in this paper.

AS	Arakawa–Schubert
COARE	Coupled Ocean–Atmosphere Response Experiment
CSH	Convective–stratiform heating
ECMWF	European Centre for Medium-Range Weather Forecasts
EM	Ensemble mean
FSU	Florida State University
GARP	Global Atmospheric Research Program
GATE	GARP Atlantic Tropical Experiment
GSM	Global Spectral Model
ITCZ	Intertropical convergence zone
KWAJEX	Kwajalein Experiment
PR	Precipitation radar
RMS	Root-mean-square
SCSMEX	South China Sea Monsoon Experiment
SE	Superensemble
TOGA	Tropical Ocean and Global Atmosphere
TMI	TRMM Microwave Imager
TRMM	Tropical Rainfall Measuring Mission
ZM	Zhang–McFarlane

of cumulus parameterization schemes in large-scale models. Furthermore, it has also been recognized that error from a cumulus parameterization can be model dependent; that is, the rest of the model physics and dynamics can dictate a particular behavior of the cumulus parameterization scheme within a particular model. Nonhydrostatic models that include microphysical processes can carry sensitivities specific to microphysical processes and can also exhibit similar model dependencies. For hurricane simulations, the modeling of the vertical level of maximum heating and its amplitude were recognized to be fairly important (Ooyama 1969; Ceselski 1974). Convection plays a major role in tropical intraseasonal variability and quasi-stationary circulation. Errors in the vertical placement of heating and the magnitudes of heating do have implications in the modeling of convectively coupled wave propagation such as ITCZ, MJO, and moist Kelvin waves. (A list of acronyms is provided in Table 1.) Climate models have difficulty in the simulation of MJO, and large sensitivity of such simulations to the vertical heating distributions has been noted by several authors (Slingo et al. 1996; Waliser et al. 2003; Zhang 2005; Zhang et al. 2006).

Having observed estimates of heating rates is fairly important for model validations. In a series of papers, Shige et al. (2004, 2007, 2008) have examined the vertical profiles of heating in tropical weather systems. Their studies have shown the limitations in the modeling of the vertical distribution of heating from case studies that covered Tropical Ocean and Global Atmosphere Coupled Ocean–Atmosphere Response Experiment (TOGA COARE) and Global Atmospheric Research Program (GARP) Atlantic Tropical Experiment (GATE) events. Lau et al. (2000) and Johnson and Ciesielski (2002) have pioneered examining vertical distribution of heating using field experiment datasets, especially those from South China Sea Monsoon Experiment (SCSMEX). Yuter et al. (2005) have studied the diurnal change of latent heating within the context of the Tropical Rainfall Measuring Mission (TRMM) Kwajalein Experiment (KWAJEX).

2. Superensemble methodology

The superensemble methodology combines a set of multimodel forecasts to construct a single consensus forecast (Krishnamurti et al. 1999, 2000). In this methodology, the models are combined with different weights, which is unlike a simple ensemble construction. The weights of the models are determined based on their past performance. The details of this methodology are as follows.

The time line of the model dataset is divided into two parts: a training phase and a forecast phase. In the training phase, the models are compared with the observation–analysis data. A multiple linear regression is performed in this phase to estimate the relative performance of the member models. The outcome of this regression is statistical weights assigned to each of the models. These weights are then passed on to the forecast phase to construct the superensemble forecast:

$$S = \overline{O} + \sum_{i=1}^{N} a_i (F_i - \overline{F_i}), \tag{1}$$

where $\overline{O}$ is the observed mean field during the training phase; a_i is the weight for the ith member model; F_i and $\overline{F_i}$ are the forecasts and mean forecast fields during the training phase from the ith model. The summation is taken over the N member models of the suite. The calculation of the weights are done by multiple linear regression, which minimizes the error term

$$G = \sum_{t=1}^{N_{\text{tr}}} (S'_t - O'_t)^2, \tag{2}$$

where N_{tr} is the number of time samples in the training phase, and S'_t and O'_t are the superensemble and observed field anomalies, respectively, at training time t.

This exercise is performed for every grid point and vertical level in the dataset during every forecast phase. In other words, one weight is given to every model at every grid point in the three-dimensional space for each forecast.

The weights of the superensemble vary geographically and with forecast lead time. This allows the incorporation of the information on the geographical distribution of model performances within their respective weights. The superensemble forecast is different from the conventional bias-removed ensemble mean forecast; in the latter case the weights to the models are $1/N$, where N is the number of models in the suite. It was shown by Stefanova and Krishnamurti (2002) and Chakraborty and Krishnamurti (2006) that superensemble performs better than bias-removed ensemble mean forecast for short-to-medium range as well as for seasonal time-scale predictions.

3. Satellite-based heating rates

The observational estimates for the vertical profile diabatic heating rate (Q1) were derived from the TRMM Microwave Imager (TMI) instrument. This version ''b'' of the convective–stratiform heating rates (CSH) was constructed from 3G68 gridded rainfall obtained from TMI, precipitation radar (PR), and from echo-top height data from the TRMM PR (Tao et al. 2006). The horizontal resolution of the dataset is 0.5° in both longitude and latitude directions, and the data are available from 1 January 1998 to 31 December 2007 on a daily time scale. In north–south, the dataset covers the entire TRMM domain: 37°S–37°N. There are 19 levels in the vertical where this dataset is defined. The vertical levels start at 0.5 km; thereafter the levels are at 1, 2, and 3 through 18 km at intervals of 1 km. The data coverage from TRMM for one day (2 July 2007) of orbit and for two consecutive days (2 and 3 July 2007) is illustrated in Fig. 1. The coverage for two days shows the precession of the TRMM orbit. The one-day coverage leaves some data-void squares within which the heating rates are not directly available. We have validated the model-based heating profiles along the orbital paths and especially at the location of these orbital intersections.

4. Model description

We have used the Florida State University (FSU) Global Spectral Model (GSM) for the calculation of vertical heating rate. This model has a triangular truncation at 170 waves (T170), which corresponds to about a 0.7° grid in both the longitude and latitude directions near the equator. The model has 27 vertical sigma levels with more closely spaced levels near the surface and at the tropopause. The details of this model are presented in Krishnamurti et al. (2007).

Three different cumulus convection parameterization schemes were used within the FSU GSM to construct multimodels. These three schemes have entirely different physical basis for convection parameterization. These schemes are 1) Kuo parameterization (Krishnamurti et al. 1980; Krishnamurti and Bedi 1988), 2) simple Arakawa–Schubert parameterization (Grell 1993; Pan and Wu 1995), and 3) Zhang–McFarlane parameterization (Zhang and McFarlane 1995). Details of these parameterization schemes as used in the FSU GSM are given in Krishnamurti et al. (2008b).

The outputs of the models were obtained at every 3 h from the model start time through 60 h of forecasts. We had monitored the vertical velocity and the sea level pressure every time step, and these two variables had equilibrated by around hour 12 (for the initial day) and their variations became more monotonic at grid points, Therefore, in order to leave out model spinup, we have not used the first 12 h of forecasts to calculate skill scores. Mean fields from the period of 12–36 h are termed as day 1 in this study. Day 2 forecasts consist of the mean fields from 36 through 60 h.

5. Experimental details

Integration of these models was carried out to 60 h using each of the above cumulus convection parameterization schemes starting at 1200 UTC of 23 March 2007 through 17 July 2007 (117 days in total). The first 100 days constituted a training phase and superensemble forecasts were constructed for the last 17 days. Separate sets of regression coefficients [a_i's of Eq. (1)] were calculated for 12–36 h (day 1) and 36–60 h (day 2) of forecasts for each of the member models at each grid location.

To calculate the vertical profile of heating rate Q_1, we have used the familiar equation (Yanai et al. 1973; Krishnamurti et al. 2008a)

$$Q_1 = C_p \left(\frac{p}{p_0}\right)^{\kappa} \left(\frac{\partial \theta}{\partial t} + \mathbf{V} \cdot \nabla \theta + \omega \frac{\partial \theta}{\partial p}\right), \qquad (3)$$

where C_p is the specific heat of air in constant pressure, p is pressure at the level where Q_1 is to be calculated, p_0 is a reference pressure (taken as 1000 hPa), κ is a constant (0.286), θ is potential temperature, $\mathbf{V}$ is horizontal wind vector, ∇ is the horizontal gradient operator, and ω is vertical pressure velocity. The values of Q_1 were calculated at every vertical level and at all grid points at each 3 h of forecast interval for day 1 and day 2 forecasts.

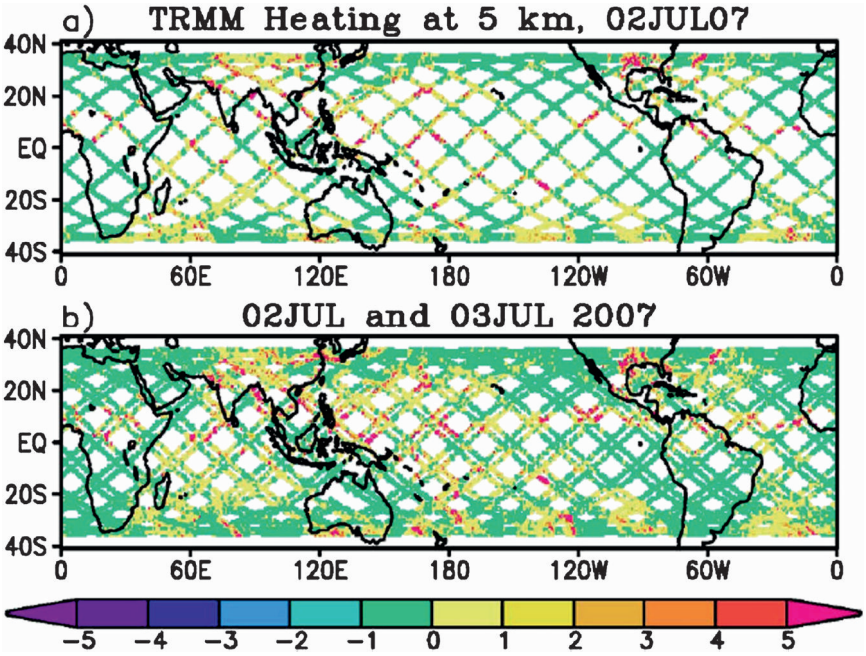

FIG. 1. Observed heating rate (Q1) from TRMM PR instrument interpolated to the model grid. (a) Spatial distribution of Q_1 on 2 Jul 2007; (b) spatial distribution of Q_1 on 2 and 3 Jul 2007 showing nonoverlapping satellite swath during consecutive days.

Averaged values of Q_1 for all the 8 time intervals during day 1 defined the model database for Q_1. Day 2 forecasts follow similarly.

To compare model-generated heating profiles and to construct superensemble forecasts, we have interpolated observed profiles of heating rates to the model grid (~0.7°) using bilinear interpolation technique. Figure 1 shows that because of the narrow swath of the TMI instrument there is a wide gap between two successive passes. This gap is greater near the equator and decreases toward the poles. Because of the precession of the TMI orbit, the full equatorial belt is covered in about 4–5 days. In other words, two consecutive passes over a grid occur only once in 4–5 days in this region. This reduces the number of effective training days on a single grid near the equator to as low as 20 out of the total 100-day period. It was shown in Mishra and Krishnamurti (2007) that the minimum number of training data points to obtain a stable set of weights is around 75 days. To avoid this problem, we have calculated a single set of weights [of Eq. (1)] for every 2 × 2 (4 in total) grid boxes. All valid observed and model data points belonging to these four boxes during the training period were used in the training phase. This increases the number of training data points. The latitudinal variation of the number of training data points along 180°E at every 2 × 2 grid box is shown in Fig. 2. Note that the total number of training data points near the equator is around 80 (as opposed to about 20). Once a set of weights is calculated for 2 × 2 grids, this is applied to all the four original model grids in the forecast phase to carry out the superensemble forecasts. This procedure allows the construction of a stable set of weights while still maintaining its geographical variations.

6. Results

a. *Predicted vertical distribution of heating*

Figure 3 illustrates an averaged vertical distribution of heating Q_1 over a summer monsoon region between 5° and 25°N and 70° and 90°E. This illustration is based on TRMM CSH datasets and multimodel forecasts for 2 July 2007. These results are for the 12–36 h averaged forecasts. Here we present vertical distribution of heating for the superensemble (SE), the ensemble mean (EM), and the results from model forecasts that utilized the following cumulus parameterization schemes: Zhang–McFarlane (ZM), the Arakawa–Schubert (AS), and the modified Kuo's scheme (Kuo). Our interest here is a feature such as the vertical level of maximum heating, the shape of the heating profile, and the maximum amplitude of heating. The heating profiles for the ZM and AS forecasts carry a maximum value near 3.5 km (above the ground). This is lower than the TRMM-based observed value, which places it at around 7.5 km. The Kuo

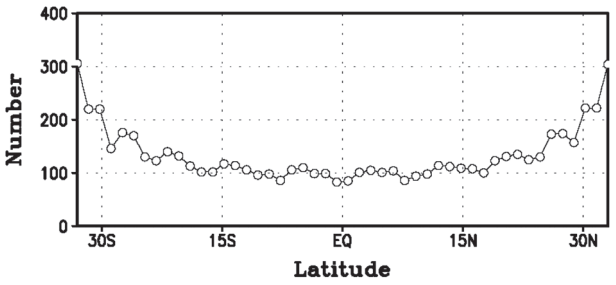

FIG. 2. Variation of number of training data points at every 2×2 grid box as a function of latitude at 180°. This variation is very similar along all other longitudes.

scheme places the maximum value near 10.5 km, which is somewhat too high compared to the TRMM estimates. The ensemble mean predicts a flat maximum between the 3- and 10-km levels. The maximum amplitude of heating for the three schemes is of the order 3 K day^{-1} (for ZM and AS) and 10 K day^{-1} (for Kuo). The ensemble mean carries a value of around 5 K day^{-1}. The TRMM-based estimate is of the order of 3 K day^{-1} and the superensemble carries a value of around 2.5 K day^{-1}. At around 17 km, a secondary maximum is predicted by all three models, which is also visible in the ensemble mean. The TRMM-based estimates above 12 km are close to zero, and that is very reasonably predicted by the multimodel superensemble. The RMS errors of these forecasts are presented in the top right of Fig. 3. The member model heating profile errors are 0.9 (for ZM), 1.1 (for AS), 5.7 (for Kuo), 2.3 (for the ensemble mean), and 0.6 (for the superensemble). It is possible to reduce the error of the vertical profile of this low value for the multimodel superensemble because of the large and consistent systematic errors in the heating profiles of the member models. Overall, we see a marked improvement for prediction of the maximum heating and the shape of the heating profiles for the superensemble.

In Fig. 4 we show daily profiles of the vertical distribution of heating Q_1 covering the period 3 July through 18 July 2007. These are averaged heating rates for the monsoon region between 5° and 25°N and 70° and 90°E. The results shown here for the forecasts are quite similar to what was seen in the previous figure. In nearly all cases the Kuo scheme overestimates the heating and places it as a level close to 9 or 10 km (above the ground). The superior performance of the multimodel superensemble, for the estimates of the heating, can also be seen from zonal vertical cross sections of Q_1 over the monsoon region in Fig. 5. In this illustration we show the isopleths of Q_1 as a function of latitude and height. These are longitudinal averages over the belt 85°–95°E, covering the period 2–18 July 2007 for day 1 of forecasts. The units are degrees K day^{-1}. The TRMM-based ''observed'' estimates are compared with the heating rates from the models using Kuo, AS, ZM, EM, and SE. We note here that the heating rates are clearly overestimated by the Kuo scheme; the other schemes show large latitudinal and vertical placement bias errors. We

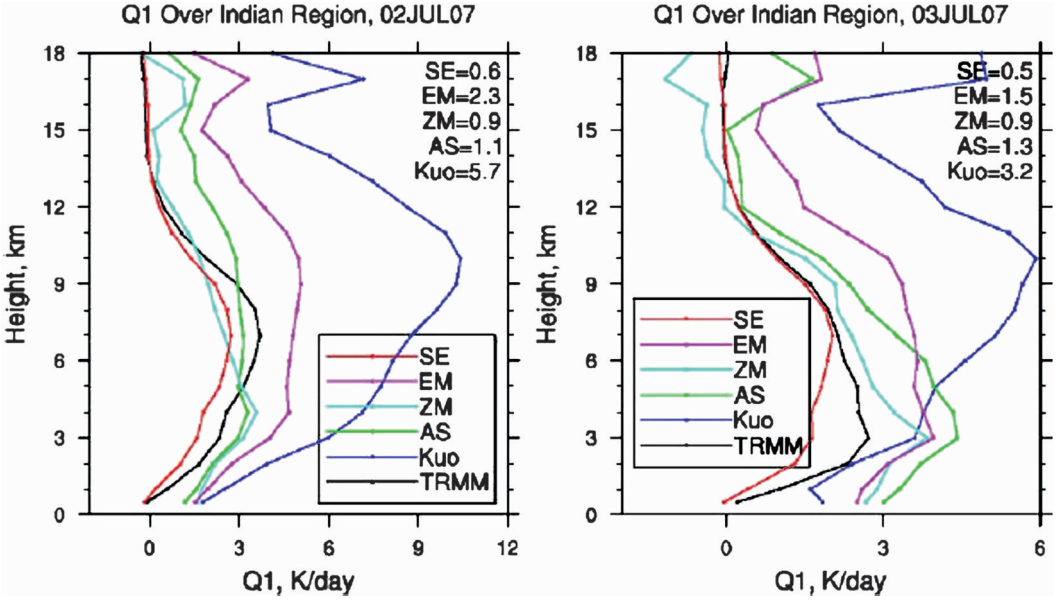

FIG. 3. Vertical profile of Q_1 from TRMM PR estimates, and forecasts of three member models, their ensemble mean and the superensemble over the Indian region (5°–25°N, 70°–90°E) during 2 Jul 2007. (left) For 12–36-h forecasts (day 1); (right) for 36–60-h forecasts (day 2). The RMS errors of the forecast fields are indicated as numbers (K day^{-1}) at the top right corner of the panels.

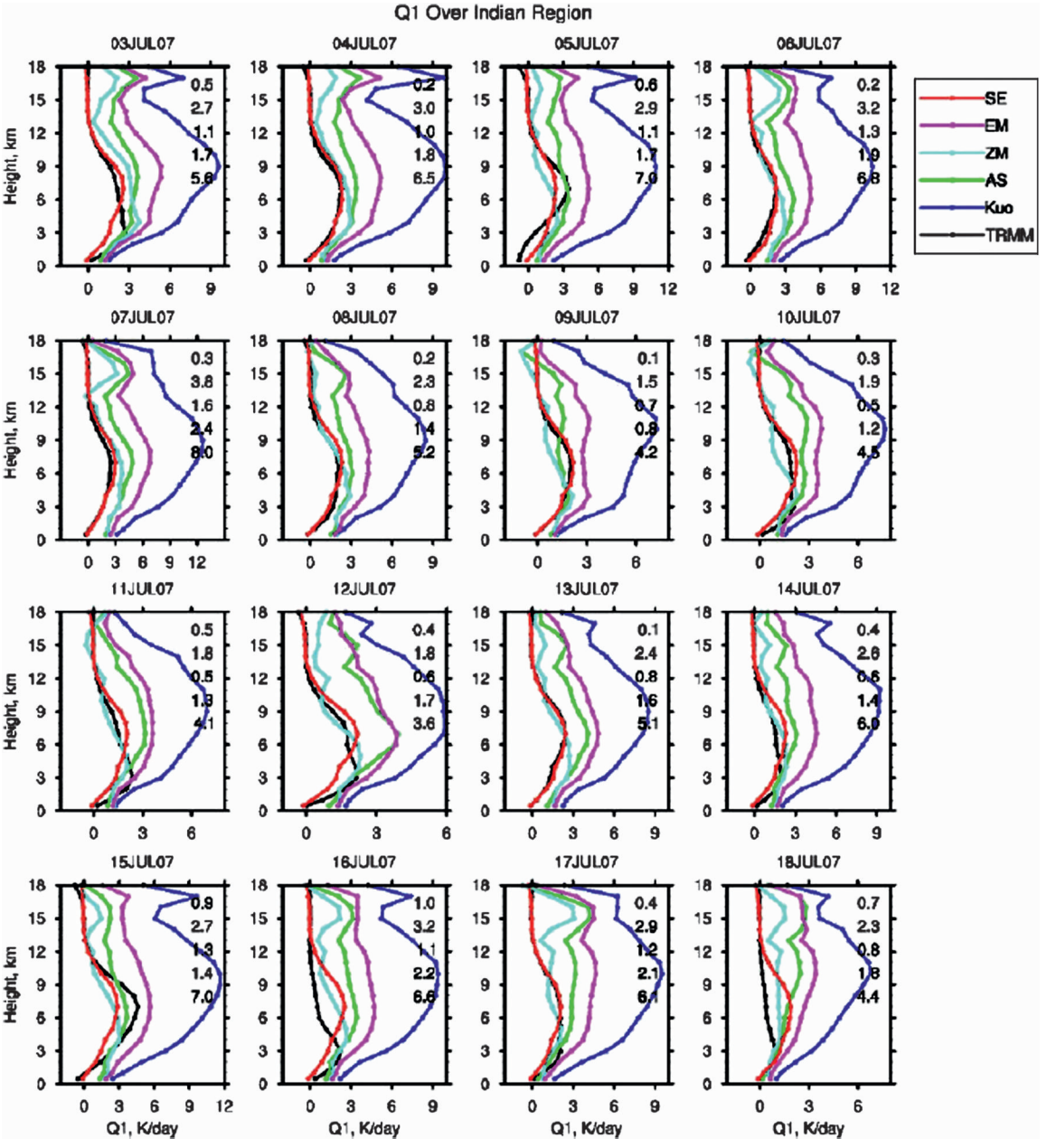

FIG. 4. Vertical profile of Q1 from TRMM PR estimates, and 12–36-h (day 1) forecasts of three member models, their ensemble mean, and the superensemble over the Indian region (5°–25°N, 70°–90°E) during 3–18 Jul 2007. The RMS errors of the forecast fields are indicated as numbers (K day^{-1}) at the top right corner of the panel.

also include the RMS errors (RMSE) and the spatial correlation (SC) error estimates for each of these forecast realizations in the top right of each panel of Fig. 5. The RMS error of the best model ZM is 4.3, which is reduced to 1.4 from the deployment of the multimodel superensemble; the pattern correlation of the best model ZM is 0.22, which is increased to 0.71 from the use of the multimodel superensemble. The performance of the ensemble mean is close to that of the best model. Over all it has been possible to improve forecasts on the heating rates from the superensemble quite drastically.

Figures 4 and 5 clearly show that the AS and ZM schemes carry a more reasonable heating, but those are still overestimates compared to the TRMM-based estimates. The superensemble reduces a large part of these errors. The RMS error of the vertical profile of the heating (Q_1) is less than 1 K day^{-1} for these forecasts. Thus it is possible to reduce the errors in the forecasts of

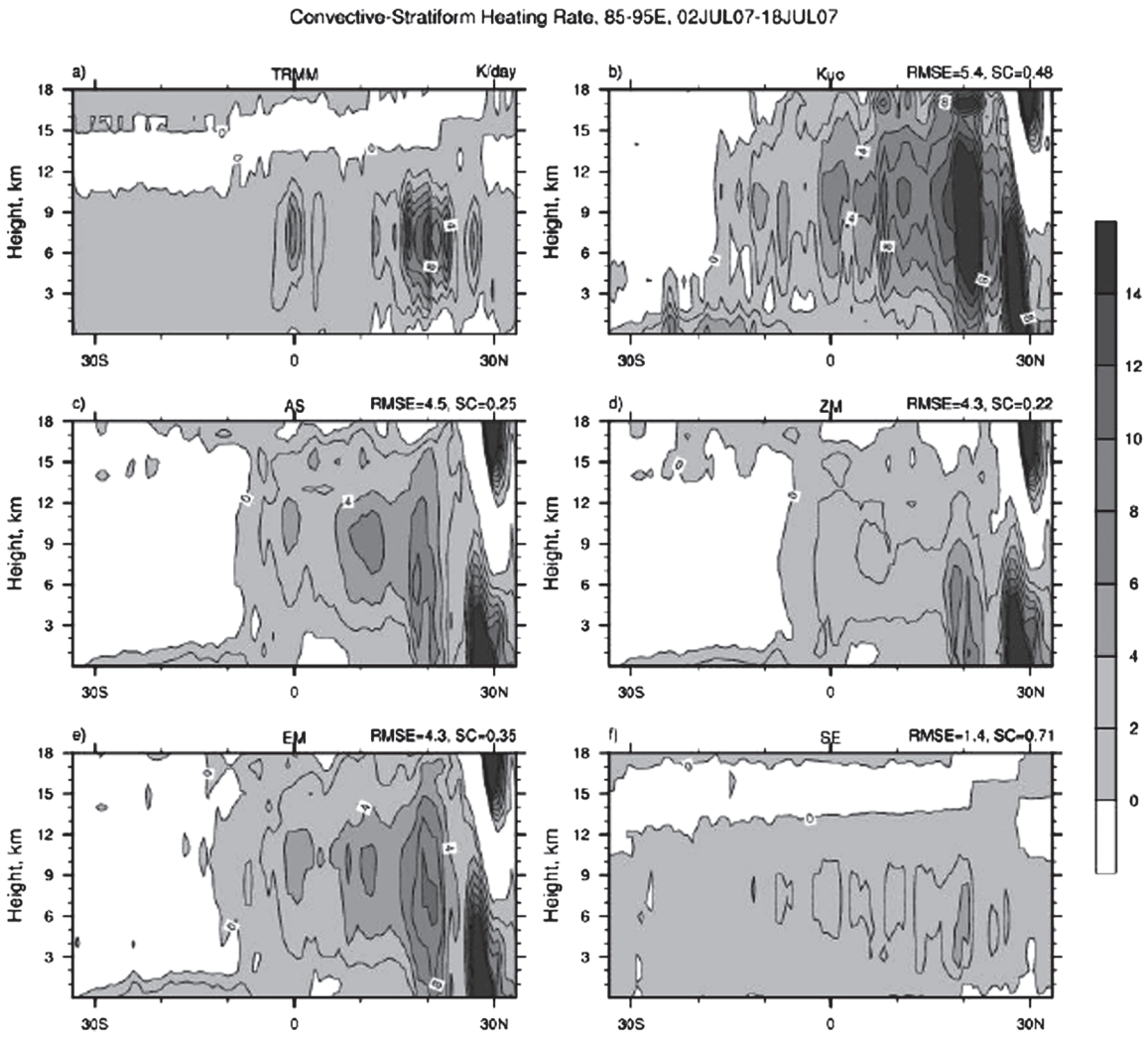

FIG. 5. Zonally averaged vertical cross section of heating profile (Q_1) from TRMM PR estimates, and 12–3-h (day 1) forecasts of three member models, their ensemble mean, and the superensemble (between 85° and 95°E), during 2–18 Jul 2007. The RMS errors and spatial correlations of the forecast fields are indicated as numbers (K day^{-1}) at the top right corner of the panel.

the amplitude and the vertical level of the heating Q_1 from the construction of the multimodel superensemble. It is possible to explore errors that arise from different components (dynamics or physics) of a single member model, such as the cumulus parameterization, by a statistical method (Krishnamurti et al. 1996). Thus a combination of the results on systematic errors as revealed by the superensemble and the error tagging from the methodology of Krishnamurti et al. (1996) would be an important next step.

b. Geographical distributions of the amplitudes of maximum heating

In this section we illustrate in Figs. 6 and 7 the time-averaged maximum values of heating along the vertical from the TRMM CSH–observed estimates and those from the model forecasts. The results presented here are the maxima of heating based on forecasts for the period 2–18 July 2007. The two diagrams show, respectively, the predicted maxima of heating distributions for hours 12–36 and hours 36–60. The units of heating are here expressed in K day^{-1}. The first 12 hours are not included in the analysis presented here; for reasons of the initial spinup within the three models that utilize different convection schemes, those are different from the Tiedtke (1989) mass flux scheme, which was implicit in the data assimilation that defines our initial states and came from the European Centre for Medium-Range Weather Forecasts (ECMWF) model. The spinup was there for several reasons; we did not carry out data assimilation with each of our models, we simply borrowed the assimilated initial fields from the ECMWF. The

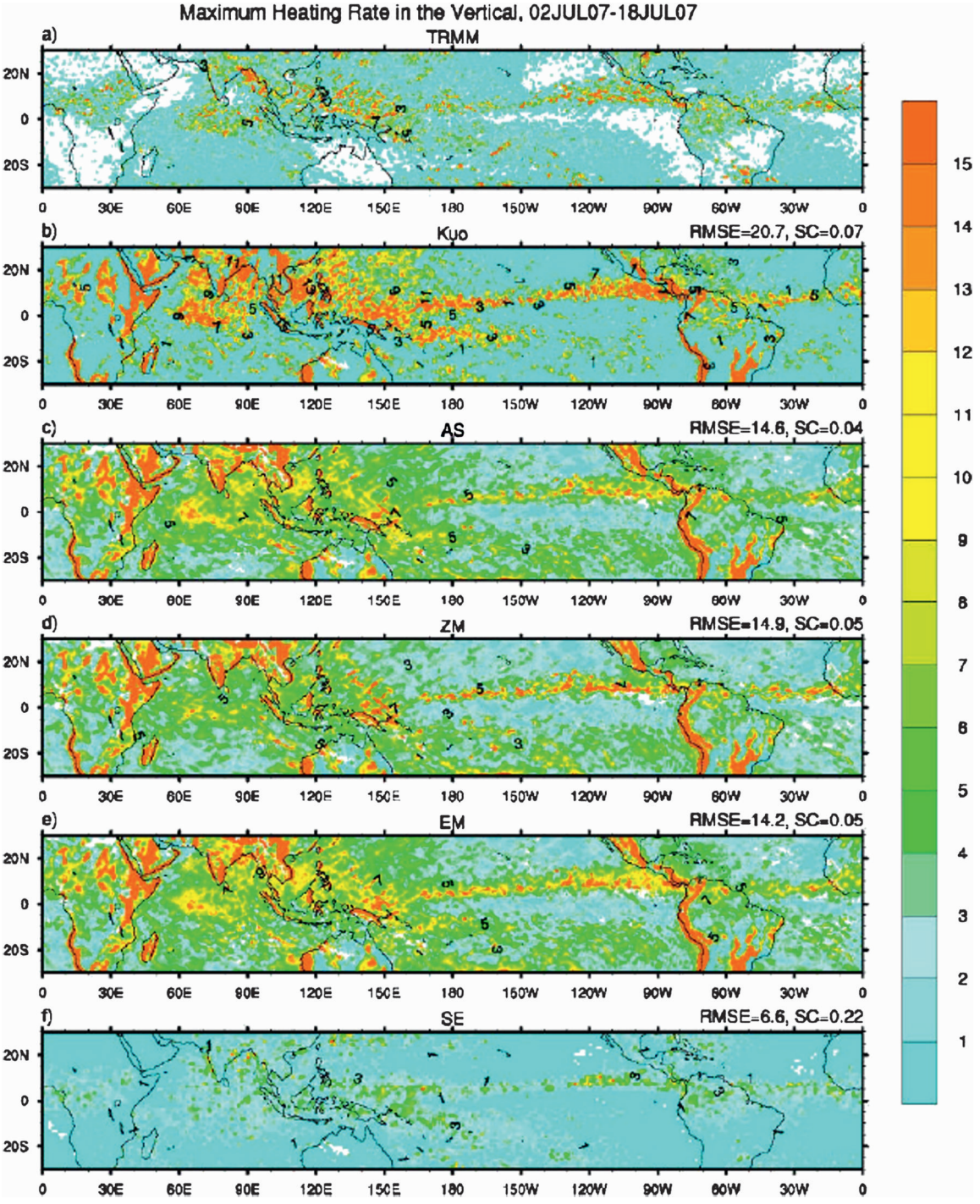

FIG. 6. Maximum vertical heating rate (Q_1) from TRMM PR estimates, and 12–36-h forecasts of three member models, their ensemble mean, and the superensemble over the Indian region during 2–18 Jul 2007. RMS errors and spatial correlations of the forecast fields are indicated as numbers at the top right corner of the panel.

model differences in physics, dynamics, and resolution all contribute to such an initial spinup. Vertical velocity and the sea level pressure had equilibrated by hour 12, and their variations were more monotonic at grid points; this gave us enough confidence to conclude that roughly 12 h were needed to pass up this initial spinup. In each of Figs. 6 and 7 we present 6 panels; these in sequence are the TRMM-based heating estimates and the results from

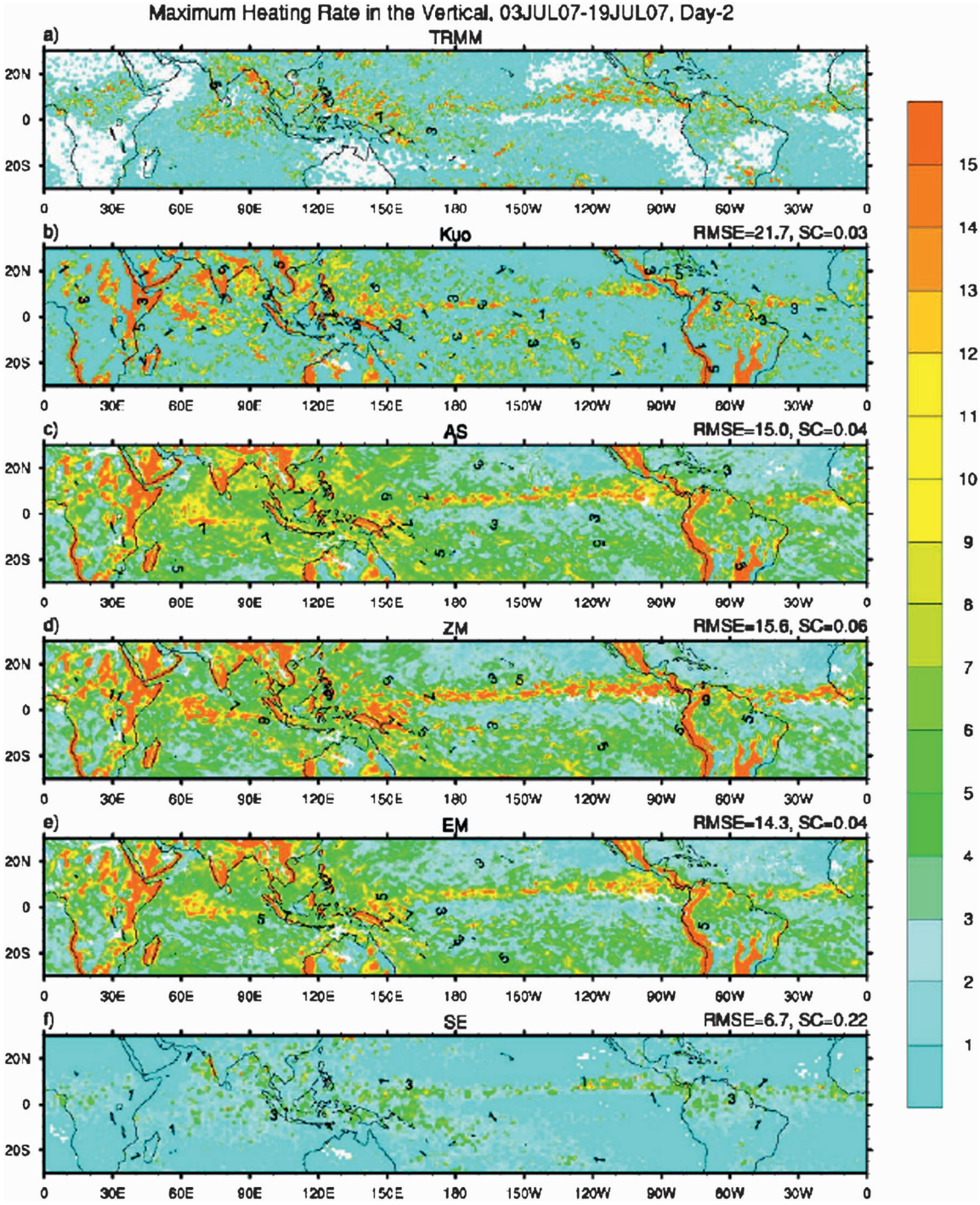

FIG. 7. Maximum vertical heating rate (Q_1) from TRMM PR estimates, and 36–60-h forecasts of three member models, their ensemble mean, and the superensemble over the Indian region during 3–19 Jul 2007. RMS errors and spatial correlations of the forecast fields are indicated as numbers at the top right corner of the panel.

the three FSU models that include the Kuo, AS, and the ZM cumulus parameterization schemes. The last two panels include results of forecasts from the ensemble mean and the multimodel superensemble. It is clear from these two figures that the maxima of the heating rates from the TRMM-based estimates are generally much lower than the estimates from the three models. Models, in general, overestimate the maximum of heating

over Africa, the Asian monsoon, and over the ITCZ. The ensemble means also reflect the member models and provide an overestimate. These overestimates can be large by a factor of 2 in many regions. Larger values of the model heating rates show a spread along major rainfall belts compared to the spread of large heating from the TRMM-based estimates. The multimodel superensemble shows a geographical distribution of maximum heating that is closest to the TRMM-based estimates. The member models clearly carry large consistent systematic errors in heating; those are corrected by the superensemble. Overall this exercise was useful in identifying the behavior of the three cumulus parameterization schemes within the FSU global model. That behavior, as we had stated earlier, may vary from model to model. The vertical placement of the level of maximum heating is next discussed.

c. *Level of maximum heating*

Figures 8 and 9 are a continuation of the previous section and all fields are similarly presented in terms of the period, the TRMM-based products, the model forecasts, the ensemble mean, and the superensemble. Here we show the geographical distributions of the vertical level of maximum heating. The TRMM-based levels of maximum heating are in general very low compared to the forecasts from the member models and their ensemble mean. These overestimates of the level of maximum heating occur over the entire tropics. This appears to be a major mismatch between model and TRMM-based results. The models place the level of maximum heating between 9 and 14 km in most places. A lot of those are nonrainy areas, such as the subtropical highs. The regions colored white in the TRMM-based estimates are nonrainy areas where no data were available. Over these regions the discrepancies arise from other components of physical parameterization such as the radiative transfer. These are large systematic errors that seemed consistent from one day to the next. Over the major rain areas of the Asian summer monsoon and the ITCZ the discrepancies are not that large. The multimodel superensemble, by correcting for these consistent systematic errors, is able to provide the best forecasts for the level of maximum heating over all areas of the tropics. Thus it has been possible to obtain the best forecasts for the amplitude of maximum heating and for the level of maximum heating for the construction of the multimodel superensemble forecasts. Included in Figs. 6–9 are the RMS errors (presented on the top right) for each forecast using the TRMM-based product as our benchmark.

Member model results seem to show a large difference from the TRMM-based heating rates. The large difference between the observed and model-forecasted vertical level of maximum heating may not be due to only the flaw in the cumulus parameterization schemes; this might well reflect shortcomings in the observed heating rates implied by the TRMM profiling methodology. The heating profile output from the model and TRMM are simply not compatible at high latitudes. This is reflected very clearly over weakly precipitating regions where the differences between the TRMM-based heating rates differ most from the model estimates. In a complex GCM where every component affects the others it is always difficult to pinpoint the reasons for deficiencies. However, since cumulus parameterization is mainly responsible for precipitation in a GCM, and it is precipitation that largely determines the maximum level of heating rate in absence of elevated land (orography), it may be argued that a large portion of the error in the model is due to the deficiencies of the cumulus parameterization schemes.

Figure 10 shows a comparison of model and TRMM-based precipitation. Here the day 2 (36–60 h) forecasts from 3 to 19 July 2007 are averaged for the three member models (AS, ZM, and Kuo) individually and plotted along with mean precipitation from TRMM-3B42 three-hourly precipitation product over the same time period. Average precipitation over the tropics for the period (3–19 July 2007) is placed on the top right corner of each plot. For comparison to the TRMM-3B42 observed precipitation each model's day 2 forecasts RMSE and spatial correlation are presented at the bottom left side of each model's panel. It is clear that the AS forecasts carried the least RMS error and a maximum spatial correlation in comparison to the ZM and Kuo forecasts. However, they all failed to realistically forecast the rainfall intensity reasonably; even the best model's average forecast (4.97 mm) is almost twofold higher than the observed TRMM averages precipitation (2.55 mm). The Kuo parameterization–based average rain (9.41 mm) forecasts are almost 4 times the observed (TRMM) rain, it carried a maximum RMS error (9.72 mm) and the lowest spatial correlation (0.60) among all the three models. Models fail to provide realistic forecast (especially Kuo model) over the global tropics and over the monsoon region in particular. Several of our previous studies show improvements in precipitation forecasts using FSU multimodel superensemble (Krishnamurti et al. 2008b, 2009).

Figure 11 shows an example of mean precipitation from the model forecasts for difference intervals of the TRMM estimated precipitation rates (mm day^{-1}). Here we have used day 2 forecasts of the model that utilized the Kuo, ZM, and AS cumulus parameterization schemes. Light precipitation is generally overestimated by the model forecasts. The model precipitation is less compared to the TRMM estimates for precipitation

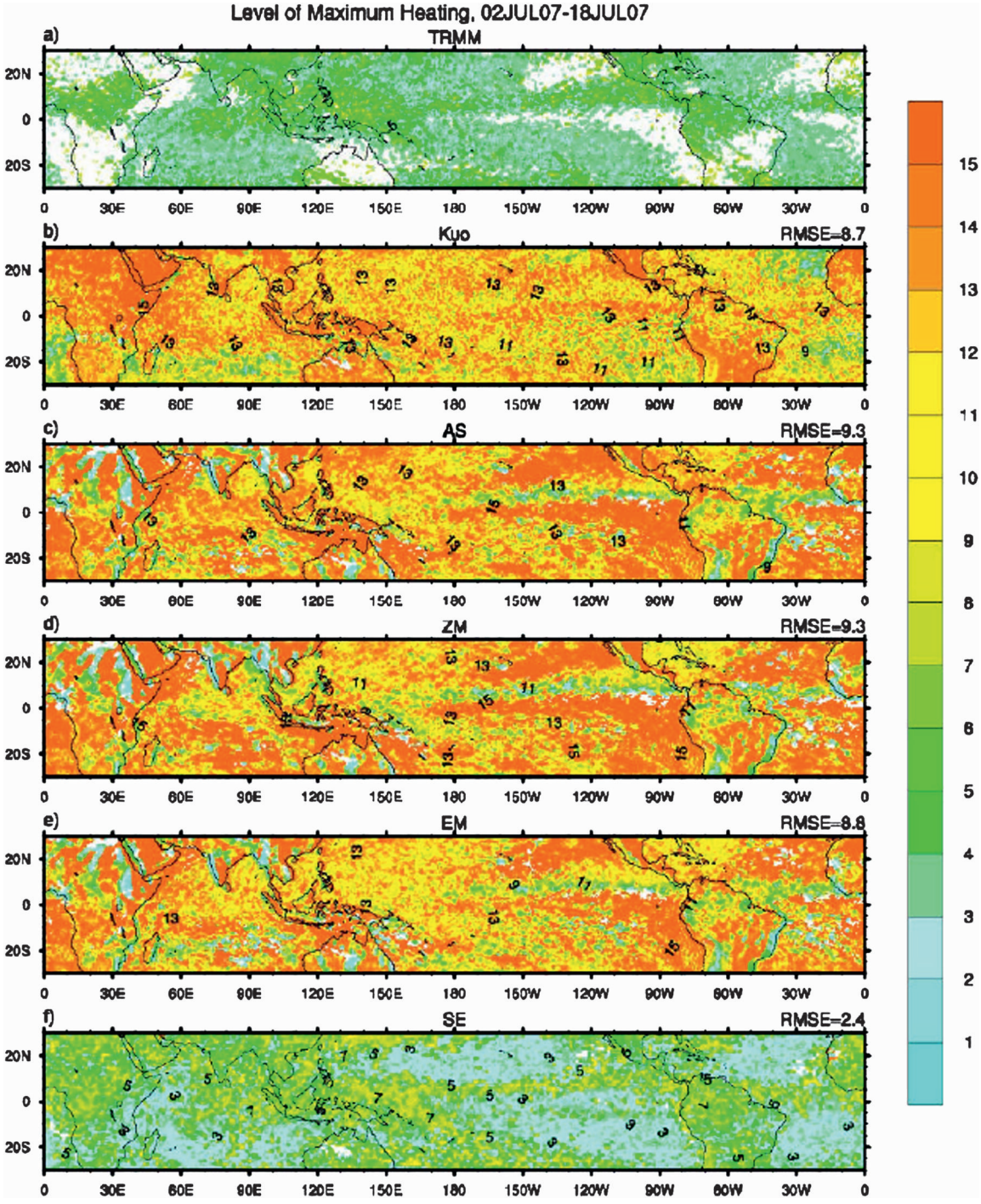

FIG. 8. Vertical level (km) of maximum heating (Q_1) from TRMM PR estimates, and 12–36-h forecasts of three member models, their ensemble mean, and the superensemble over the Indian region during 2–18 Jul 2007. RMS errors of the forecast fields are indicated as numbers at the top right corner of the panel.

ranges more than 10 mm day^{-1} for the ZM and AS schemes, and is more than 20 mm day^{-1} for the Kuo scheme. All the three parameterization schemes overestimate low precipitation rates, the Kuo scheme showing the largest errors. This figure clearly shows why the model's level of maximum heating is much different from the TRMM estimates over regions of low precipitation rates.

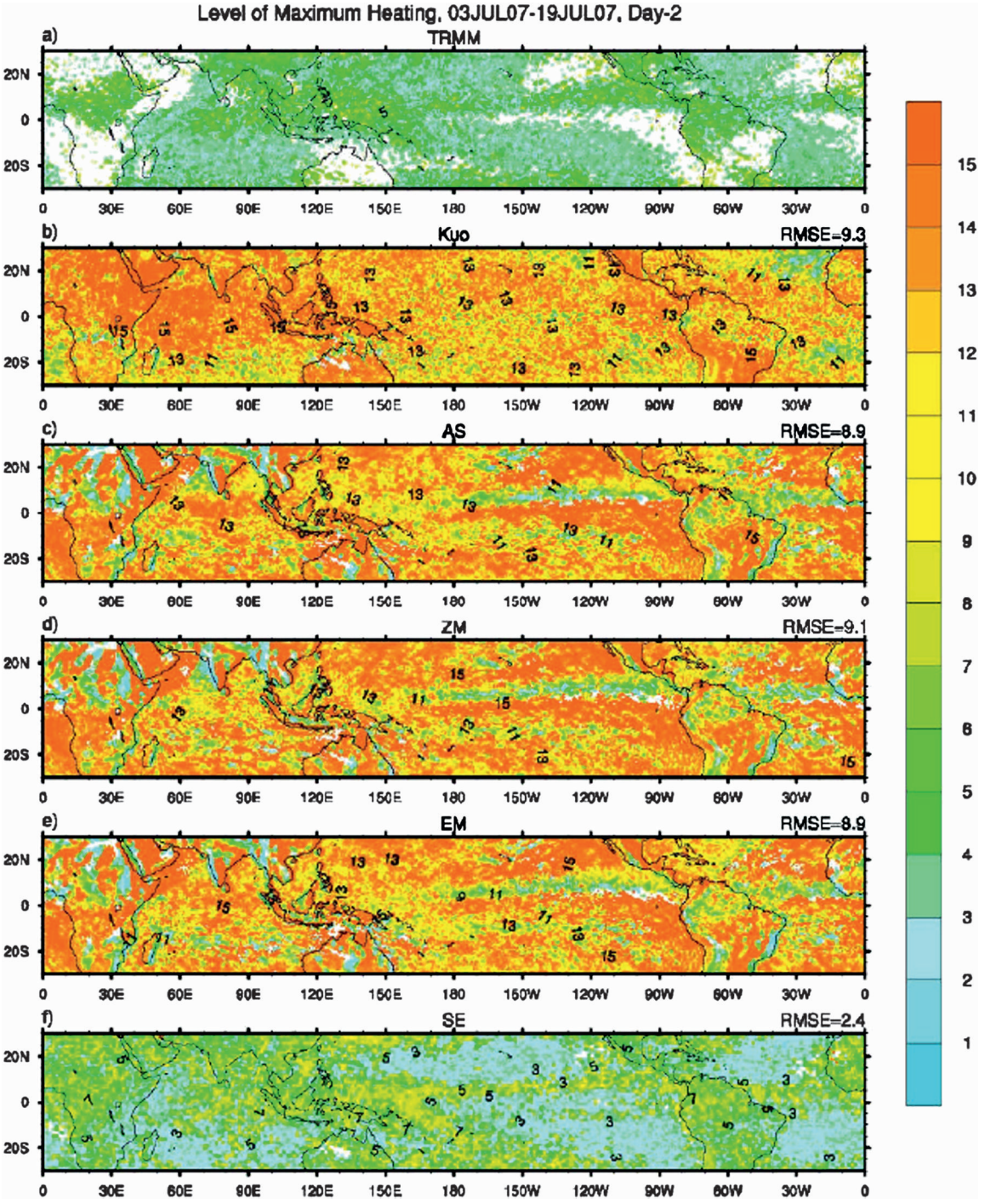

FIG. 9. Vertical level (km) of maximum heating (Q_1) from TRMM PR estimates, and 36–60-h forecasts of three member models, their ensemble mean, and the superensemble over the Indian region during 3–19 Jul 2007. RMS errors of the forecast fields are indicated as numbers at the top right corner of the panel.

The forecast improvements shown in Figs. 3–9 are indeed very marked from the use of the multimodel superensemble. These improvements are of the order of factors of 2 to 3 for the RMS errors and for the spatial correlations. Since the superensemble provides us with forecasts for all variables at all vertical levels, these heating parameters are an integral part of those forecast fields and can be used for a variety of useful diagnostic studies.

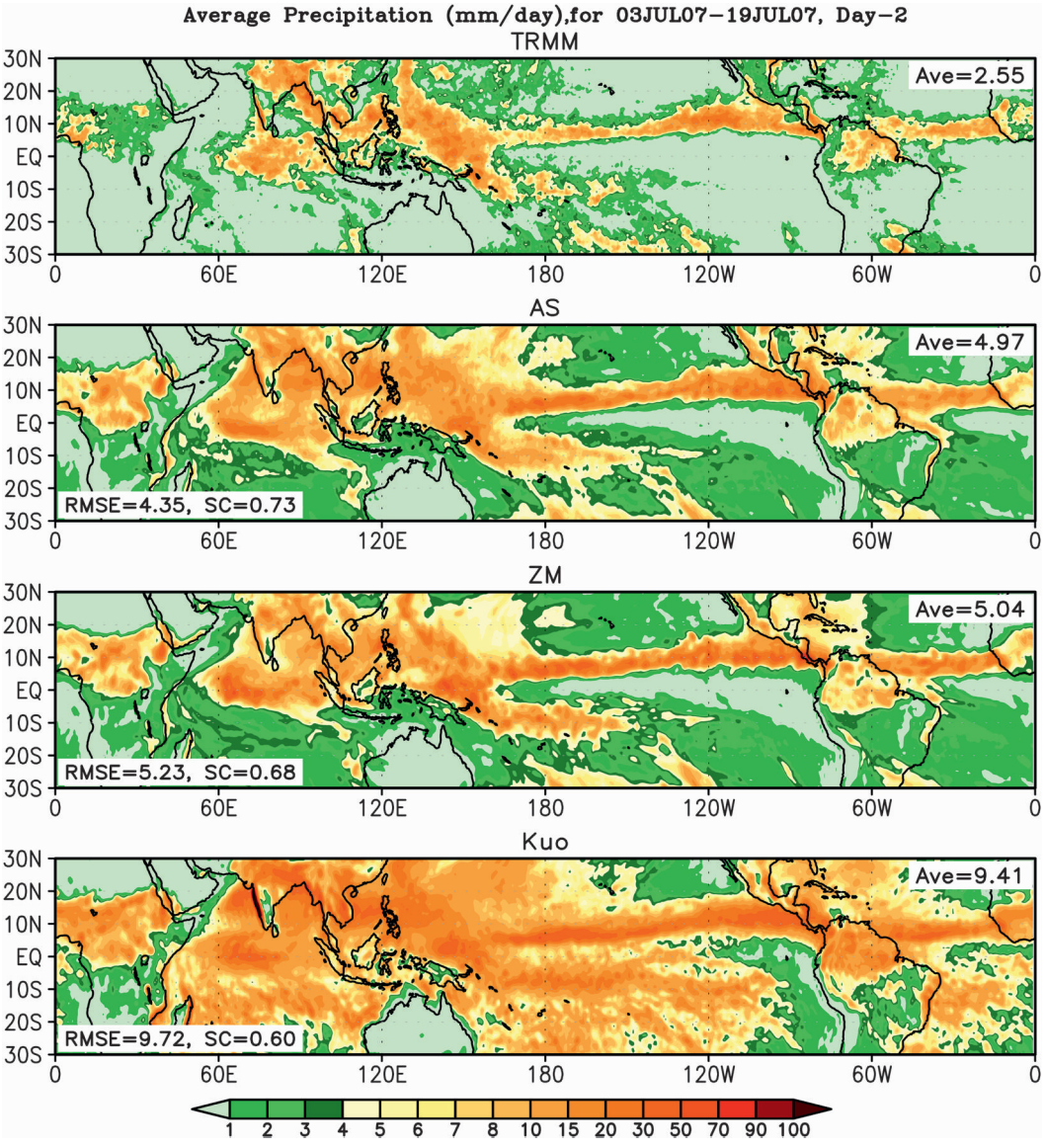

FIG. 10. Average total precipitation from three member models (day 2 forecasts) and TRMM-based 3B42 product over the global tropics during 3–19 Jul 2007. RMS errors and pattern correlations of the forecast fields along with average are indicated as numbers at the bottom left and top right corner of the panel.

7. Concluding remarks and future work

We have shown in this paper that we can reduce the systematic errors of the heating (amplitudes, vertical level of maximum heating, the shape of the heating profile in the vertical, and the geographical distributions) from the construction of a multimodel superensemble of a suite of models. These member models utilized different cumulus parameterization schemes. All of these member models were identical in their dynamical and physical parameterizations (except for the cumulus parameterization). They carry same number of vertical levels and same formulations of surface and other processes including resolution, orography, and initial states. Using nearly 100 experiments from each of these member models, during the training phase of the multimodel superensemble we were able to obtain the systematic biases for their diabatic heating representations. The multimodel superensemble exploits these collective bias errors of the member models and reduces them. We show here that for a large number of forecasts we can drastically reduce these errors in the vertical and geographical distributions and the amplitude of the errors of the member models from the multimodel

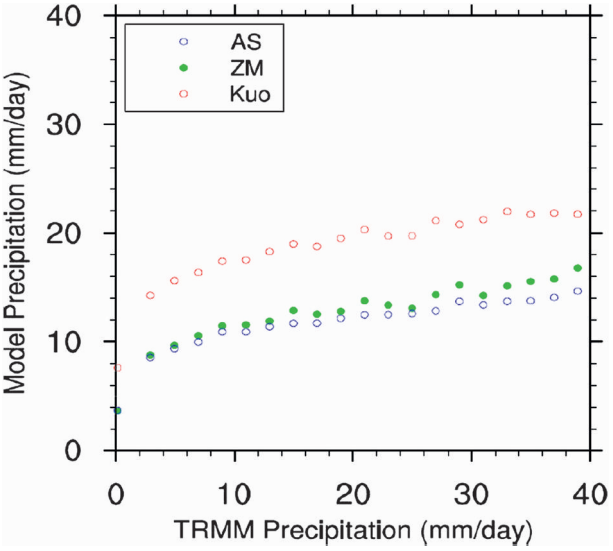

FIG. 11. Mean precipitation (mm day^{-1}) at different intervals over the tropics (30°S–30°N, 0°–360°E) from TRMM (3B42) estimates and FSU GSM's day 2 forecasts during 3–19 Jul 2007 from Kuo, ZM, and AS cumulus parameterization schemes.

superensemble. Since the superensemble can provide forecasts for all the variables including the heating and other functions of model variables (only Q_1 superensemble is carried out in this paper), we have useful products here that can be exploited for a variety of postprocessing studies with these datasets.

Examining the vertical profiles of heating (Q_1), we noted that the Kuo scheme consistently provided overestimates for the amplitude of the heating and placed the heating at a higher level compared to the TRMM-based observed estimates. The corresponding values from the AS and the ZM schemes were slightly overestimated and were placed at a slightly lower level compared to the TRMM-based estimates. The RMS errors in these predicted vertical profiles of heating were reduced to values as low as 0.1–0.5 K day^{-1} as compared to the best model, which carried RMS errors of the order of 1.1–2.2 K day^{-1}. The geographical distributions of the RMS errors for the amplitude of the maximum heating for the superensemble was around 6.6 K day^{-1} as compared to the best model, which carried an RMS error of around 14.2 K day^{-1}. These RMS errors were generally similar for forecasts between 12 and 60 h. The geographical distribution of RMS errors for the level of maximum heating was reduced to roughly 2.4 km compared to the best model, which carried an RMS error of roughly 8.8 km. While looking at the geographical distributions of these heating errors we noted that over nonprecipitating areas large errors in heating Q_1 arise from the radiative transfer algorithms. The nature of these errors were very persistent, that is, systematic, and the multimodel superensemble was able to reduce these errors quite drastically.

The strength of this study reconfirms the great strength of the multimodel superensemble. In a series of papers (Yun et al. 2003; Chakraborty and Krishnamurti 2006; Krishnamurti et al. 2006; Stefanova and Krishnamurti 2002) we have recently shown that it is possible to reduce the deterministic and probabilistic errors, from the use of the multimodel superensemble, for seasonal forecasts compared to those of as many as 13–15-member models of our suite of global coupled models. These were the state-of-the-art models from Europe, the United States, and Canada. The variables that we had examined in this series of papers include precipitation, surface air temperatures, 850-hPa-level winds, and the SST anomalies. The success of the multimodel superensemble lies in its ability to reduce persistent systematic errors of these member models. In the climate modeling context we use as many as 10^7 statistical weights for the reduction of errors. That large number comes from a product of the grid points in the three dimensions times the number of models, times the number of variables that are handled. These weights (fractional, negative, or positive) vary geographically, vertically, by the model, and by the variable. The present paper suggests that a further reduction of errors may be possible for the seasonal climate forecasts if we also include a reduction of the systematic errors for the vertical distribution of heating.

The most important aspect of this exercise has been the diagnosis of the model errors on the placement and amplitudes of heating of the member models. That information can be very useful for addressing possible corrections for the various cumulus parameterization schemes used in our study. In this context we also recognize that the behavior of a particular physical parameterization algorithm also depends to a certain extent on the particular model within which it resides. The rest of the model's physics, dynamics, and resolution also dictate the mode of behavior of a particular physical parameterization scheme. Nevertheless, we feel that the information we can obtain from this type of modeling can still be quite useful. Following Krishnamurti and Sanjay (2003) we can also construct a single unified model that utilizes the statistical weights of the multimodel superensemble for the heating. Such an exercise has been carried out previously by us for a choice of different cumulus parameterization (Krishnamurti and Sanjay 2003), for different planetary boundary layer formulations (Krishnamurti et al. 2008a), and for different cloud radiative transfer algorithms (Chakraborty et al. 2007). In each such design of a single unified model

we noted that it is possible to obtain higher skills for the respective processes compared to any of the single member models. It is thus possible to design a single unified model that utilizes the heating functions based on the weights of a multimodel superensemble. Such a model would carry the least errors for the three-dimensional placements of the heating and their amplitudes. Ideally, the design of a single model carrying the highest skill forecasts is necessary. That requires much further work in almost all areas of model physics, dynamics, and data assimilation. This work is in progress and will be reported separately.

Acknowledgments. The CSH dataset was provided by Drs. W.-K. Tao, W. Lau, J. Wu, and S. Lang. This study was supported by Grants NASA PMM-NNX07AD39G and NSF ATM-0419618. We wish to convey our thanks to Dr. W.-K. Tao for encouraging us to carry out this study. The reviewers' comments greatly helped us in improving the manuscript.

REFERENCES

Ceselski, B. F., 1974: Cumulus convection in weak and strong tropical disturbances. *J. Atmos. Sci.,* **31,** 1241–1255.

Chakraborty, A., and T. N. Krishnamurti, 2006: Improved seasonal climate forecasts of the South Asian summer monsoon using a suite of 13 coupled ocean–atmosphere models. *Mon. Wea. Rev.,* **134,** 1697–1721.

——, ——, and C. Gnanaseelan, 2007: Prediction of the diurnal cycle using a multimodel superensemble. Part II: Clouds. *Mon. Wea. Rev.,* **135,** 4097–4116.

Grell, G. A., 1993: Prognostic evaluation of assumptions used by cumulus parameterization. *Mon. Wea. Rev.,* **121,** 764–787.

Johnson, R. H., and P. E. Ciesielski, 2002: Characteristics of the 1998 summer monsoon onset over the northern South China Sea. *J. Meteor. Soc. Japan,* **80,** 561–578.

Krishnamurti, T. N., and H. S. Bedi, 1988: Cumulus parameterization and rainfall rates: Part III. *Mon. Wea. Rev.,* **116,** 583–599.

——, and J. Sanjay, 2003: A new approach to the cumulus parameterization issue. *Tellus,* **55,** 275–300.

——, Y. Ramanathan, H. L. Pan, R. J. Pasch, and J. Molinary, 1980: Cumulus parameterization and rainfall rates I. *Mon. Wea. Rev.,* **108,** 465–472.

——, H. Bedi, G. Rohaly, and D. Oosterhof, 1996: Partitioning of the seasonal simulation of a monsoon climate. *Mon. Wea. Rev.,* **124,** 1499–1520.

——, C. M. Kishtawal, T. E. LaRow, D. R. Bachiochi, Z. Zhang, C. E. Williford, S. Gadgil, and S. Surendran, 1999: Improved weather and seasonal climate forecasts from multimodel superensemble. *Science,* **285,** 1548–1550.

——, ——, Z. Zhang, T. E. LaRow, D. R. Bachiochi, C. E. Williford, S. Gadgil, and S. Surendran, 2000: Multimodel superensemble forecasts for weather and seasonal climate. *J. Climate,* **13,** 4196–4216.

——, A. Chakraborty, R. Krishnamurti, W. K. Dewar, and C. A. Clayson, 2006: Seasonal prediction of sea surface temperature anomalies using a suite of 13 coupled atmosphere–ocean models. *J. Climate,* **19,** 6069–6088.

——, C. Gnanaseelan, and A. Chakraborty, 2007: Prediction of the diurnal cycle using a multimodel superensemble. Part I: Precipitation. *Mon. Wea. Rev.,* **135,** 3613–3632.

——, S. Basu, J. Sanjay, and C. Gnanaseelan, 2008a: Evaluation of several different planetary boundary layer schemes within a single model, a unified model and a multimodel superensemble. *Tellus,* **60A,** 42–61.

——, C. Gnanaseelan, A. K. Mishra, and A. Chakraborty, 2008b: Improved forecasts of diurnal cycle in tropics using multiple global models. Part I: Precipitation. *J. Climate,* **21,** 4029–4043.

——, A. K. Mishra, A. Chakraborty, and M. Rajeevan, 2009: Improving global model precipitation forecasts over India using downscaling and FSU superensemble. Part I: 1–5-day forecasts. *Mon. Wea. Rev.,* **137,** 2713–2735.

Lau, K. M., and Coauthors, 2000: A report of the field operations and early results of the South China Sea Monsoon Experiment (SCSMEX). *Bull. Amer. Meteor. Soc.,* **81,** 1261–1270.

Mishra, A. K., and T. N. Krishnamurti, 2007: Current status of multimodel superensemble and operational NWP forecast of the Indian summer monsoon. *J. Earth Syst. Sci.,* **116,** 369–384.

Ooyama, K. V., 1969: Numerical simulation of the life cycle of tropical cyclones. *J. Atmos. Sci.,* **26,** 3–40.

Pan, H.-L., and W. S. Wu, 1995: Implementing a mass flux convection parameterization package for the NMC medium range forecast model. NMC Office Note, Tech. Rep. 409, 40 pp.

Shige, S., Y. Takayabu, W. Tao, and D. Johnson, 2004: Spectral retrieval of latent heating profiles from TRMM PR data. Part I: Development of a model-based algorithm. *J. Appl. Meteor.,* **43,** 1095–1113.

——, ——, ——, and C. Shie, 2007: Spectral retrieval of latent heating profiles from TRMM PR data. Part II: Algorithm improvement and heating estimates over tropical ocean regions. *J. Appl. Meteor. Climatol.,* **46,** 1098–1124.

——, ——, and ——, 2008: Spectral retrieval of latent heating profiles from TRMM PR data. Part III: Estimating apparent moisture sink profiles over tropical oceans. *J. Appl. Meteor. Climatol.,* **47,** 620–640.

Slingo, J. M., and Coauthors, 1996: Intraseasonal oscillations in 15 atmospheric general circulation models: Results from an AMIP diagnostic subproject. *Climate Dyn.,* **12,** 325–357.

Stefanova, L., and T. N. Krishnamurti, 2002: Interpretation of seasonal climate forecast using Brier skill score, FSU superensemble, and the AMIP-I data set. *J. Climate,* **15,** 537–544.

Tao, W.-K., and Coauthors, 2006: Retrieval of latent heating from TRMM satellite measurements. *Bull. Amer. Meteor. Soc.,* **87,** 1555–1572.

——, J. R. A. Houze, and E. Smith, 2007: The fourth TRMM latent heating workshop. *Bull. Amer. Meteor. Soc.,* **88,** 1255–1259.

Tiedtke, M., 1989: A comprehensive mass flux scheme for cumulus parameterization in large-scale models. *Mon. Wea. Rev.,* **117,** 1779–1800.

Waliser, D. E., and Coauthors, 2003: AGCM simulations of intraseasonal variability associated with the Asian summer monsoon. *Climate Dyn.,* **21,** 423–446.

Yanai, M., S. Esbensen, and J.-H. Chu, 1973: Determination of bulk properties of tropical cloud clusters from large-scale heat and moisture budgets. *J. Atmos. Sci.,* **30,** 611–627.

Yun, W.-T., L. Stefanova, and T. N. Krishnamurti, 2003: Improvement of the multimodel superensemble technique for seasonal forecasts. *J. Climate,* **16,** 3834–3840.

Yuter, S., J. R. A. Houze, E. Smith, T. Wilheit, and E. Zipser, 2005: Physical characterization of tropical oceanic convection observed in KWAJEX. *J. Appl. Meteor.,* **44,** 385–415.

Zhang, C., 2005: Madden-Julian Oscillation. *Rev. Geophys.,* **43,** RG2003, doi:10.1029/2004RG000158.

——, M. Dong, H. H. Hendon, E. D. Maloney, A. Marshall, K. R. Sperber, and W. Wang, 2006: Simulations of the Madden–Julian oscillation in four pairs of coupled and uncoupled global models. *Climate Dyn.,* **27,** 573–592, doi:10.1007/s00382-006-0148-2.

Zhang, G. J., and N. A. McFarlane, 1995: Sensitivity of climate simulations to the parameterization of cumulus convection in the Canadian Climate Centre general circulation model. *Atmos.–Ocean,* **33,** 407–446.